Ukrainian Journal of Physical Optics
ISSUE 4
2026

THE INFLUENCE OF QUANTUM PARTICLE MASS ON THE DISCRETE ENERGY SPECTRUM OF MULTILAYER STRUCTURES: A FOURIER TRANSFORM APPROACH

V. FITIO, I. YAREMCHUK, M. SHCHETININ*, M. HLADUN, P. STAKHIRA

Department of Electronic Engineering, Lviv Polytechnic National University, 12 S. Bandery str., 79013, Lviv, Ukraine
*Corresponding author: mykhailo.s.shchetinin@lpnu.ua

Received: 14.04.2026

Abstract. Many optoelectronic devices contain multilayer structures with quantum wells, particularly semiconductor lasers and light-emitting structures based on organic semiconductors (OLEDs). The stationary Schrödinger equation must be solved to determine the discrete energy levels in quantum wells. This must account for the fact that the effective mass of carriers in different layers differs. The paper analyses a structure comprising three quantum wells of different widths, in which the charge-carrier effective masses differ. We propose a numerical method for solving the Schrödinger equation in the frequency domain. This method considers the different effective masses in quantum wells and barriers. The obtained discrete energy levels were compared with those calculated using the de Broglie wave method. This made it possible to determine the parameters of the numerical process required to achieve high accuracy. Studies have shown that the mass of particles in barriers has little effect on discrete energy levels, whereas the mass of particles in quantum wells has a significant impact. Numerical calculations have demonstrated that for an abrupt change in particle mass at the well-barrier interface, the first derivative of the wave function satisfies the BenDaniel-Duke boundary conditions. Wave function moduli in the coordinate domain have been constructed for the lowest energy levels. This indicates strong charge carrier localization in quantum wells.

Keywords: multilayer quantum structures, Schrödinger equation, Fourier transform, de Broglie wave method, quantum particle mass
UDC: 620.9
DOI: 10.3116/16091833/Ukr.J.Phys.Opt.2026.04034

1. Introduction

Multilayer quantum structures are present in many optoelectronic devices, including semiconductor lasers [1] and light-emitting structures based on organic semiconductors [2]. Incorporating quantum wells into these structures increases the internal quantum efficiency and improves carrier confinement in light-emitting structures [3]. This leads to a reduction in the threshold pump current in semiconductor lasers based on heterostructures [3, 4]. Using quantum wells in semiconductor lasers enables single-mode lasing under high-frequency modulation, making the lasers highly effective in telecommunication systems [5–8].

Initially, light-emitting structures based on organic materials (OLEDs), comprising carrier transport and emission layers [9, 10], failed to meet the performance requirements imposed on such devices. Subsequent research aimed to improve efficiency by synthesizing novel, high-performance transport and emission materials, investigating photon-emission mechanisms, and developing OLED structures based on quantum wells and superlattices. Exploiting quantum wells has enabled the demonstration of both white-light-emitting OLEDs and OLEDs that generate light in a narrow spectral range [11–15]. Using heterostructures with quantum-well formation in inorganic semiconductor quantum-electronic devices has

substantially improved their performance. It has enhanced the electroluminescence quantum yield, which is defined as the ratio of the number of photons emitted per unit time to the electric current.

It should be noted that OLEDs containing multiple quantum wells (QWs) have superior optical properties to single-QW OLEDs. Structures incorporating QWs have lower operating voltages, improved luminance characteristics, and greater power efficiency than OLED structures without QWs [16]. This effect is evidently associated with an increase in the carrier concentration in the emission zone of cascaded QWs. Similar conclusions have been reached in other studies [2, 17, 18]. Furthermore, it is possible to form quantum wells of different widths in a series of quantum wells [19], thereby enabling emission over a broad spectral range. Engineering the barrier widths between quantum wells (QWs) improves carrier confinement prior to recombination. This enhances emission efficiency in specific spectral ranges corresponding to QWs of the appropriate width. This enables white-light emission.

Since the specific emission wavelengths are fundamentally determined by the discrete energy levels within these engineered quantum wells, an accurate theoretical model is required. Therefore, it is necessary to solve the time-independent Schrödinger equation to predict the emission spectrum of multilayer structures containing quantum wells. This equation yields the discrete energy levels and the corresponding wave functions.

There are two methods for searching for energy levels in quantum wells of multilayer structures. The Schrödinger equation can be solved either in the spatial domain using de Broglie waves [20] or in the frequency domain [21]. The first method is well established and described in standard textbooks on quantum mechanics. The second method, however, is less widely known. Nevertheless, it offers advantages when analyzing structures with many quantum wells [21]. It should also be noted that the effective masses of carriers in the various layers of a multilayer structure tend to differ, as the layers are made of different materials. The de Broglie wave method can be used to analyze carrier masses of different sizes without introducing any significant complications.

In contrast, solving the Schrödinger equation in the frequency domain [21] becomes more complicated in the case of position-dependent masses, and the corresponding matrix equation becomes more complex. It is therefore necessary to extend the method described in [21] to analyze multilayer OLED structures with different effective masses in their respective layers. If the masses of the quantum particles differ between the wells and the barriers, the wave function must remain continuous at the well-barrier interface. Furthermore, its first derivative must satisfy the BenDaniel-Duke boundary conditions [22], which are defined as follows:

$$\frac{d\Psi(x_0-0)}{m_b dx}=\frac{d\Psi(x_0+0)}{m_h dx}, \tag{1}$$

where x_0 denotes the coordinate of the well-barrier interface, m_b is the particle mass in the barrier, and m_h is the particle mass in the well.

2. Methods for determining the discrete energy levels of multilayer quantum structures under varying effective particle masses

Consider a simplified, three-well quantum structure. The wells have widths of 1, 3, and 5 nm, respectively, as illustrated in Fig. 1, with a 1 nm barrier width between each well. Such a structure may form part of a more complex, multilayer OLED architecture containing a

greater number of layers. It is not expected that the remaining layers will play a significant role in determining the energy levels of the quantum wells.

We adopt a one-dimensional treatment here, motivated by the following reasoning. Modern quantum devices are multilayer structures, with individual layers that are substantially thinner than 1 μm, yet with lateral dimensions that can greatly exceed this thickness. Therefore, it can be assumed that the wave function varies only in the direction normal to the plane of the layers, and not within that plane. Consequently, when analyzing such structures, it is sufficient to solve the one-dimensional, time-independent Schrödinger equation.

2.1. De Broglie wave method for analyzing multilayer quantum structures with variable particle mass

According to the de Broglie hypothesis, the momentum of a particle is given by $p=\hbar k$, where $\hbar$ is the reduced Planck constant. The wave number k is determined by the particle mass m, the potential energy U, and the total energy of the particle E according to the expression [20]:

$$k_j=\sqrt{\frac{2m_j(E-U_j)}{\hbar^2}}\quad , \tag{2}$$

It should be noted that the carriers may have different effective masses in each layer, which may be composed of different materials.

The structure under study has six jumps in potential energy (Fig. 1).

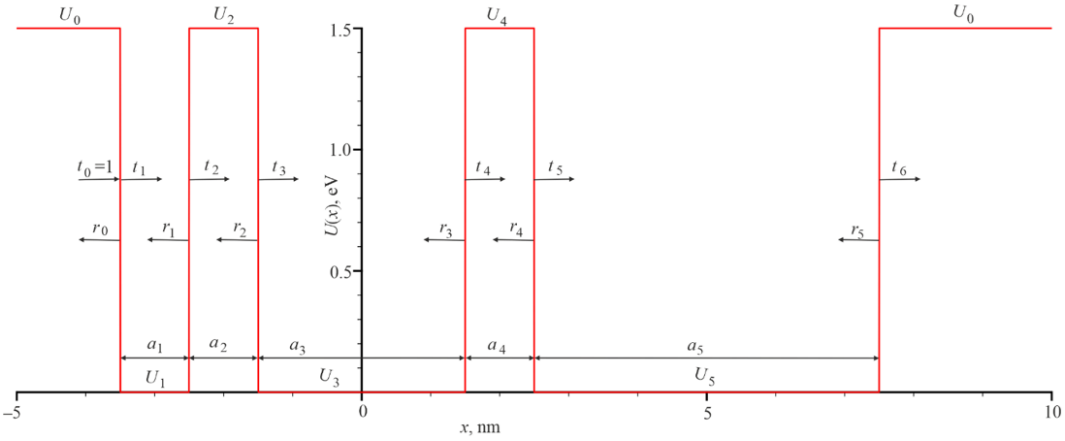

Fig. 1. System of three quantum wells with widths a_1, a_3, a_5 and two finite barriers with widths a_2 and a_4 and two barriers of infinite width with potential energy U_0.

We obtain 12 algebraic equations, considering that the wave function and its first derivatives must be continuous at the well/barrier boundaries. The unknowns are the amplitudes of the waves propagating from left to right $t_j, j=1..6$, and the amplitudes of the reflected waves from the boundaries propagating from right to left $r_j, j=0..5$.

Each QW and potential barrier corresponds to a certain mass m_j and the corresponding wave number as follows:

$$k_j=\sqrt{\frac{2m_j(E-U_j)}{\hbar^2}}, \tag{3}$$

where j varies from zero to six. Each mass m_j is conveniently written in the following form.

$$m_j = m_0/\mu_j\,, \tag{4}$$

where m_0 is the electron rest mass, and μ_j is coefficient that determines the effective mass of carrier in the corresponding layer.

Thus, the wave function depends on the particle energy, and for quantum wells and barriers, it can be expressed as follows:

$$\psi_j(x) = t_j \exp\left(ik_j x\right) + r_j \exp\left(-ik_j x\right). \tag{5}$$

Therefore, for the first interface, we can formulate the following system of two equations based on the continuity of the wave functions and the conditions specified in [22]:

$$1 + r_0 = t_1 + r_1 \exp\left(-ik_1 a_1\right) \tag{6}$$

$$i\mu_0 k_0 - i\mu_0 k_0 r_0 = i\mu_1 k_1 t_1 - i\mu_1 k_1 r_1 \exp\left(-ik_1 a_1\right). \tag{7}$$

For interfaces 2, 3, 4, and 5, a generalized system of two equations can be written in the following form:

$$t_j \exp\left(ik_j a_j\right) + r_j = t_{j+1} + r_{j+1} \exp\left(-ik_{j+1} a_{j+1}\right), \tag{8}$$

$$i\mu_j k_j t_j \exp\left(ik_j a_j\right) - i\mu_j k_j r_j = i\mu_{j+1} k_{j+1} t_{j+1} - i\mu_{j+1} k_{j+1} r_{j+1} \exp\left(-ik_{j+1} a_{j+1}\right). \tag{9}$$

In Eqs. (8) and (9), for the second interface *j*=1, for the third interface *j*=2, for the fourth interface *j*=3, and for the fifth interface *j*=4. The system of equations for the sixth interface takes the following form:

$$t_5 \exp\left(ik_5 a_5\right) + r_5 = t_6\,, \tag{10}$$

$$i\mu_5 k_5 t_5 \exp\left(ik_5 a_5\right) - i\mu_5 k_5 r_5 = i\mu_6 k_6 t_6\,. \tag{11}$$

Based on Eqs. (6) – (11), we construct a system of linear algebraic equations with a non-zero right-hand side, which takes the following form:

$$\mathbf{Az = b}\,. \tag{12}$$

The matrix **A** has dimensions of 12×12, which corresponds to twice the number of interfaces and, consequently, to the number of unknowns t_j and r_j from which the vector **z** is constructed. The first two components of the vector **b** are equal to 1 and $i\mu_0 k_0$ according to Eq's. (6) and (7), while all remaining components of this vector are zero.
Thus, the unknown vector z can be determined based on the following algebraic equation:

$$\mathbf{z = A^{-1}b}\,, \tag{13}$$

where $\mathbf{A^{-1}}$ is the inverse matrix, so that $\mathbf{A^{-1} \times A} = 1$.

Based on the solution, we will construct the $t_1(E), t_3(E)$ and $t_5(E)$ to find the discrete energy levels of the QWs system. At certain values of *E*, the corresponding values of t_j will increase sharply by several orders of magnitude compared to unity. At the same values of *E*, r_j also increase sharply. These *E* values can be interpreted as discrete energy levels for a given system of QWs and barriers. Therefore, the discrete energy levels that correspond to the wave functions of maximum amplitude for three QWs are identified.

2.2. Solution of the stationary Schrödinger equation in the frequency domain with variable particle mass

The discrete levels of electrons and holes in QWs were calculated using the one-dimensional stationary Schrödinger equation [20], which is slightly modified in the presence of different

masses in the quantum wells and barriers, taking the following form [22]:

$$-\frac{\hbar^2}{2}\frac{d}{dx}\left(\frac{1}{m(x)}\frac{d}{dx}\right)\psi(x)+U_0(x)\psi(x)=E_0\psi(x), \tag{14}$$

where, $\hbar=h/2\pi$, h is the Planck constant, $m(x)$ is the mass of the quantum particle, $\psi(x)$ is the wave function, $U_0(x)$ is the potential energy in which the quantum particle is located, E_0 is the energy of the particle. In our case, $m(x)$ in the multilayer structure changes according to expression (5).

This equation was modified by multiplying both sides by $2m_0/\hbar^2$. The dimensionless Eq. (6) can be presented as:

$$-\frac{d\mu(x)}{dx}\frac{d\psi(x)}{dx}-\mu(x)\frac{d^2\psi(x)}{dx^2}+U(x)\psi(x)=E\psi(x), \tag{15}$$

where $U(x)=\frac{2m_0}{\hbar^2}U_0(x)$, $E=\frac{2m_0}{\hbar^2}E_0$.

The solution of the stationary Schrödinger equation $\psi(x)$ corresponds to discrete energy levels, and their primary derivatives tend to zero at $x\to\pm\infty$. Therefore, the Fourier transform for these functions and their primary and secondary derivatives exists, which are equal [23]:

$$\psi(u)=\mathcal{F}\{\psi(x)\}=\int_{-\infty}^{\infty}\psi(x)\exp(-i2\pi ux)dx, \tag{16}$$

$$\mathcal{F}\left\{\frac{d\psi(x)}{dx}\right\}=i2\pi u\psi(u), \tag{17}$$

$$\mathcal{F}\left\{\frac{\partial^2\psi(x)}{\partial x^2}\right\}=-(2\pi u)^2\psi(u). \tag{18}$$

In the expression for $\mu(x)$, we separate the constant and variable components. Thus, in accordance with Fig. 1, we can write: $\mu(x)=\mu_b+\tilde{\mu}(x)$. Therefore, the Fourier transform of $\mu(x)$ and the derivative $\mu(x)$ can be written in the following form:

$$\mathcal{F}\{\mu(x)\}=M(u)=\mu_b\delta(u)+\mathcal{F}\{\tilde{\mu}(x)\} \tag{19}$$

$$\mathcal{F}\left\{\frac{d\mu(x)}{dx}\right\}=\mathcal{F}\left\{\frac{d\tilde{\mu}(x)}{dx}\right\}=i2\pi u\tilde{M}(u) \tag{20}$$

In addition, if there is a Fourier transform of two functions $g(x)$ and $h(x)$, i.e., $\mathcal{F}\{g(x)\}=G(u),\mathcal{F}\{h(x)\}=H(u)$ then the following relation is valid [23]:

$$\mathcal{F}\{g(x)h(x)\}=\int_{-\infty}^{\infty}G(u-v)H(v)dv, \tag{21}$$

where $\mathcal{F}\{...\}$ denotes the Fourier transform of a totally integrable function, u,v are the coordinates in the frequency domain the Fourier transform of a totally integrable function is defined. Eq. (21) describes the content of the convolution theorem.

As a result of the Fourier transform of both parts of Eq. (15) using (16-21), the following equation was obtained:

$$4\pi^2\int_{-\infty}^{\infty}(u-v)\tilde{M}(u)v\psi(v)dv+4\pi^2\int_{-\infty}^{\infty}M(u-v)v^2\psi(v)dv+\int_{-\infty}^{\infty}U(u-v)\psi(v)dv=E\psi(u), \quad (22)$$

where $M(u)=\mathcal{F}\{\mu(x)\},U(u)=\mathcal{F}\{U(x)\}$.

Therefore, the transition was made from the differential Eq. (15) for eigenfunctions (i.e., wave functions in the coordinate domain) and eigenvalues (i.e., corresponding to discrete energy levels) to the integral (22). In this equation, the integral can be replaced by a sum and the continuous variables by discrete ones. The following expression is obtained because of these transformations:

$$\begin{aligned}&4\pi^2\sum_{p=-(N-1)/2}^{(N-1)/2}(s\Delta-p\Delta)\tilde{M}(s\Delta-p\Delta)p\Delta\psi(p\Delta)\Delta\\&+4\pi^2\sum_{p=-(N-1)/2}^{(N-1)/2}M(s\Delta-p\Delta)(p\Delta)^2\psi(p\Delta)\Delta\\&+\sum_{p=-(N-1)/2}^{(N-1)/2}U(s\Delta-p\Delta)\psi(p\Delta)\Delta \;=\; E\psi(s\Delta),\end{aligned} \quad (23)$$

where $\Delta=u_{\max}/N$, $u\to u_s=s\Delta$, $v\to v_p=p\Delta$, $-(N-1)/2\le s,p\le(N-1)/2$; s, p and N are integers, $u_{\max}$ should be taken so that at frequencies $|u|\ge u_{max}/2$ the values $\psi(u)$ are almost equal to zero [24, 25]. Also, according to the counting theorem, it is necessary to choose $x_{\max}$ such that the wave function $\psi(x)$ for $|x|\ge x_{\max}/2$ is practically equal to zero for discrete energy levels. The following relations are valid [23]:

$$|x|\ge\frac{x_{\max}}{2\Delta}=\frac{1}{x_{\max}},\; U_{\max}=N\Delta,\; x_{\max}u_{\max}=N. \quad (24)$$

The value of N must be sufficiently large (as will be shown below, N must be greater than 1000) to minimize the calculation error and should preferably be an odd number. Obviously, the sum in Eq. (23) should have N elements.

Let us write the last Eq. (15) for all discrete spatial frequencies $u_s=s\Delta$ with s varying from $\frac{-(N-1)}{2}$ to $\frac{(N-1)}{2}$. Then the set of these equations in the number N can be written as a matrix equation, with E being common to all s:

$$(Q_1+Q_2+Q_3)\Psi=E\Psi, \quad (25)$$

where the elements of the matrix $\mathbf{Q_1}$ are respectively equal to $q_1^{s,p}=4\pi^2(s\Delta-p\Delta)\tilde{M}(s\Delta-p\Delta)p\Delta^2$. The elements of matrix $\mathbf{Q_2}$ are given by $q_2^{s,p}=4\pi^2M(s\Delta-p\Delta)(p\Delta)^2\Delta$. The elements of the matrix $\mathbf{Q_3}$ are equal to $q_3^{s,p}=U(s\Delta-p\Delta)\Delta$. The column vector Ψ consists of elements $\psi(s\Delta)$ in the frequency domain, where s ranges from $-(N-1)/2$ to $(N-1)/2$ thus comprising N elements. By performing the discrete inversive Fourier transform, we obtain the ψ function in the coordinate representation.

Therefore, in Eq. (25), the function Ψ is the discrete Fourier transform of a wave function corresponding to a discrete energy level E, and must be valid according to the postulates of quantum mechanics. In cases involving several eigenvalues and their associated eigenvectors, the eigenfunction, denoted by the symbol $\psi(x)$ is obtained by taking the

inverse discrete Fourier transform of the eigenvector. In quantum mechanical problems, all the discrete energy levels lie within the potential well. If we have a potential well of finite depth, the accuracy is determined by N and Δ. As N increases and Δ decreases, accuracy increases, but this will require more calculation time.

In order to obtain wave functions in the coordinate domain, the inverse discrete Fourier transform must be performed according to the following expression:

$$\psi_j\left(m\frac{x_{\max}}{N}\right)=\sum_{n=-\frac{N-1}{2}}^{n=\frac{N-1}{2}}\exp\left(i2\pi\frac{nu_{\max}}{N}\frac{mx_{\max}}{N}\right)C_j\psi_j(n\Delta)\Delta, \tag{26}$$

where j is the number of the wave function corresponding to the discrete energy level with the same number; $j=0$ for the lowest energy level; C_j is the normalizing factor n; and m are integers that vary from $-(N-1)/2$ to $(N-1)/2$.

It should be noted that the eigenvectors of the matrix Eq. (25) $\psi_j(n\Delta)$ are orthonormal, i.e., the scalar product is given by:

$$\psi_j\psi_k=\delta_{j,k}, \tag{27}$$

where $\delta_{j,k}$ is the Kronecker delta.

The normalizing factor Cj in formula (26) can be found from the following equation:

$$\left|C_j\right|^2\sum_{n=-\frac{N-1}{2}}^{n=\frac{N-1}{2}}\left|\psi_j(n\Delta)\right|^2\Delta=1. \tag{28}$$

Considering equality (19), we find that

$$C_j=\left|C_j\right|=\frac{1}{\sqrt{\Delta}}. \tag{29}$$

Formula (26), taking into account expression (29) can be written in the following compact form:

$$\psi_j\left(\frac{m}{v_{\max}}\right)=\sum_{n=-\frac{N-1}{2}}^{n=\frac{N-1}{2}}\exp\left(i2\pi\frac{nm}{N}\right)\psi_j(n\Delta)\sqrt{\Delta}. \tag{30}$$

The wave functions in the coordinate domain are defined by formula (28) and are orthonormal. This formula will be used to calculate the wave functions for the corresponding discrete energy levels.

It should be noted that the de Broglie wave method is exact. Any errors arising from the numerical calculation are related to the number of decimal places used. The second method is asymptotically exact; that is, it is exact as N approaches infinity. Clearly, we use the matrix Eq. (25) for finite N. Therefore, the error in the calculation results has two components: rounding error and error due to the limitedness of N. It is therefore important to investigate how the calculated energies in the second method depend on N, and to choose N such that the second component of the error can be neglected.

3. Results and Discussion

The results of calculations using the first and second methods are shown in Table 1. The second method determines discrete energy levels as functions of N. The width of the barriers between quantum wells is 1 nm, $x_{\max}=50$ nm.

Table 1. Dependence of the lowest discrete energy levels for QWs with widths of 1, 3, and 5 nm for particle mass $m = m_0$.

Well width, nm	1	3	5	–
De Broglie wave method				
E, eV	0.213595	0.034116	0.013290	
Method for solving the Schrödinger equation in the frequency domain				N
E, eV	0.213675	0.034122	0.013292	501
E, eV	0.213619	0.034118	0.013291	751
E, eV	0.213604	0.034117	0.013290	1001
E, eV	0.213597	0.034116	0.013290	1501
E, eV	0.213595	0.034116	0.013290	2001

Results obtained by the second method coincide with those calculated by the first method at $N = 2001$. Therefore, all subsequent numerical calculations are performed at $N = 2001$.

The dependencies of the lowest discrete energy levels for the three wells calculated using the second method (continuous curves) and the first method (green dots) are shown in Fig. 2.

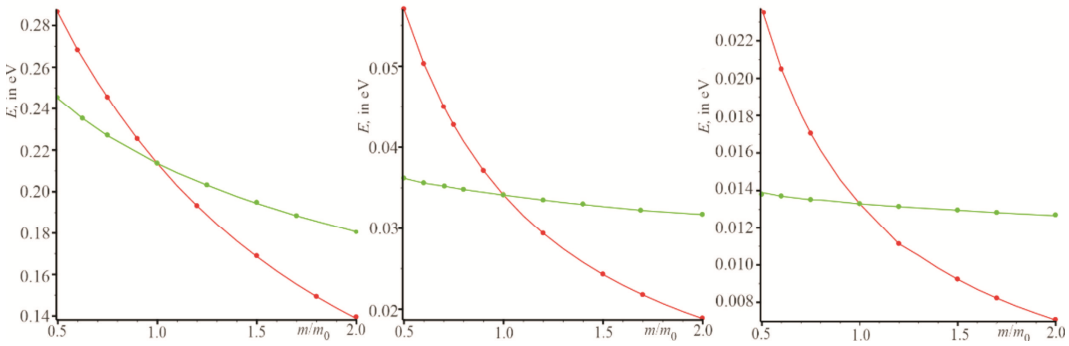

Fig. 2. Dependences of discrete energy levels on the mass of the particle in the barriers (green curves) at $m_h = m_0$ and on the mass of the particle in the wells (red curves) at $m_b = m_0$; (a) well width 1 nm, (b) well width 3 nm, (c) well width 5 nm. The continuous curves were obtained using the de Broglie wave method, while the points represent the solutions of the Schrödinger equation in the frequency domain.

As we can see, the green dots (de Broglie waves) correspond quite well to the continuous curves (the solution to the Schrödinger equation in the frequency domain). The minimum difference is observed at the lowest energy (in a 3-nm-wide QW). The greatest discrepancy between the two calculations' results is also observed at a width of 1 nm. In other words, to obtain more accurate results as E increases, it is necessary to increase $N, x_{\max}$ and $u_{\max}$, which requires more computational power and time.

It should also be noted that the discrete energy levels depend slightly on the mass of the particles within the potential barriers (green curves in Fig. 2). However, the mass of the particles in QWs has a significant impact on the discrete energy level (red curves in Fig. 2). Fig. 3 shows the moduli of the wave functions $\psi(x)$ for some values of m_h and m_b.

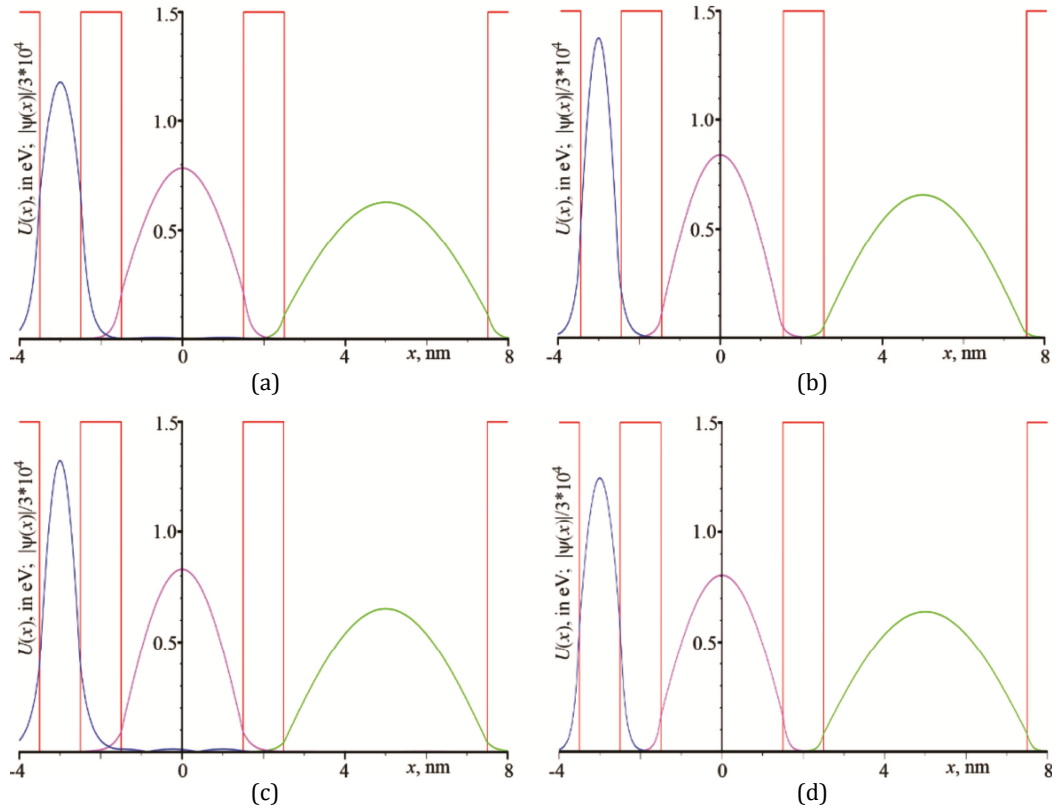

Fig. 3. Dependencies of the potential energy $U(x)$ (red curve) and the moduli of the wave functions $\psi(x)$ with localization in a well with a width of: 1 nm (blue curve), 3 nm (magenta curve), 5 nm (green curve); (a) m_h=0.5m_0 and m_b=m_0; (b) m_h=2m_0 and m_b=m_0; (c) m_h=m_0 and m_b=0.5m_0; (d) m_h=m_0 and m_b=2m_0.

As seen in Fig. 3, the wave functions are qualitatively well localized within the quantum wells. It can clearly be seen that the wave function exhibits a kink at the well-barrier interface, indicating a discontinuity in its first derivative. In this case, the BenDaniel-Duke boundary conditions are satisfied, and the quantity $\frac{d\psi(x)}{m(x)dx}$ remains a continuous function. Fig. 4 demonstrates the fulfillment of this condition. In this case, the wave function

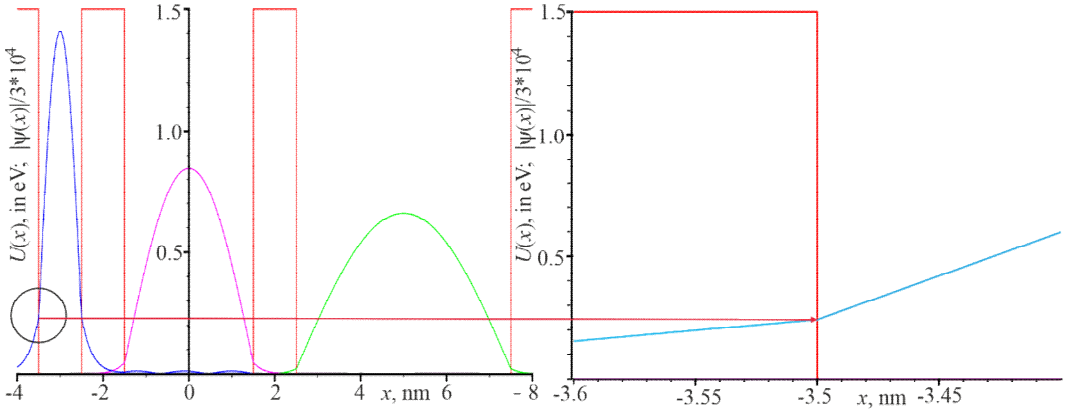

Fig. 4. The wave function modulus as a function of the x coordinate (left) and an enlarged view of the wave function modulus at the barrier-well interface (right).

calculations were performed to better visualize the BenDaniel-Duke boundary conditions for $m_h = 2m_0$ and $m_b = 0.5m_0$, namely the ratio $m_b/m_h = 1/4$. The right-hand side of Fig. 4 shows an enlarged view of the area circled on the left-hand side of the figure. A kink in the wave function is observed at the barrier-well interface, indicating that its derivative is discontinuous, while the ratio of the derivatives on the left and right sides of this interface is $1/4$ Thus, our numerical calculations show that the condition is satisfied:

$$\frac{d\psi(x_0-0)}{m_b dx} = \frac{d\psi(x_0+0)}{m_h dx}. \tag{31}$$

4. Conclusions

A new numerical method is proposed to solve the stationary Schrödinger equation in the frequency domain for multilayer quantum structures, in which the masses of the particles differ. This method is also suitable for cases involving a continuous change in particle mass. Since the wave functions and their first and second derivatives tend to zero at infinity for discrete energy levels, we can apply the Fourier transform to the stationary Schrödinger equation. As a result, we obtain an integral equation in the frequency domain. By replacing the continuous variables with discrete ones and taking the reference theorem into account, we arrive at a higher-level algebra problem involving eigenvalues and eigenvectors.

The eigenvalues represent the discrete energy levels, and the corresponding eigenvectors are the discrete Fourier images of the wave functions. Performing the inverse discrete Fourier transform yields the wave function in the coordinate domain.

The analysis focused on a multilayer structure comprising three quantum wells, each with a width of 1, 3, or 5 nm. The width of the barriers was 1 nm. The analysis showed that while the discrete energy levels depend slightly on the particle mass in the potential barriers (green curves in Fig. 2), the particle mass in the QWs has a strong effect on the discrete energy levels (red curves in Fig. 2).

It was found that changing the particle masses in the barriers and QWs does not qualitatively alter the wave functions, and the quantitative changes are insignificant. Increasing the particle masses in the barriers from $0.5m_0$ to $2m_0$ improves the particle localization in the QWs to some extent.

Numerical calculations were performed using both the de Broglie wave method and solutions to the Schrödinger equation. The results demonstrate that the BenDaniel-Duke boundary conditions are satisfied for coordinate-dependent masses, even in the case of an abrupt mass change at the barrier-well interface.

Funding and acknowledgements. The research presented in this paper was funded by the National Science Foundation (NSF) (Grant No 0124U003833).

Disclosures. The authors declare no conflict of interest.

Authors contribution. Volodymyr Fitio and Iryna Yaremchuk conceptualized the theoretical framework and established the methodology presented in this study. Iryna Yaremchuk assisted in refining the theory by verifying and reviewing the primary theoretical conclusions. Numerical calculations and data processing were performed by Volodymyr Fitio, Mykhailo Shchetinin, and Mykhailo Hladun. The manuscript was prepared and formatted for publication by Mykhailo Shchetinin. Pavlo Stakhira provided expert consultation and physical insights regarding the behavior of organic light-emitting structures and quantum wells.

References

1. Krames, M. R. (2017). Light emitting diode materials and devices. *Materials for Solid State Lighting and Displays*, 273-311.
2. Antrack, T., Kroll, M., Sudzius, M., Cho, C., Imbrasas, P., Albaladejo Siguan, M., ... & Leo, K. (2022). Optical properties of perovskite organic multiple quantum wells. *Advanced Science*, *9*(24), 2200379.
3. Hayashi, I., Panish, M. B., & Reinhart, F. K. (1971). GaAs–Al x Ga1− x As Double Heterostructure Injection Lasers. *Journal of Applied Physics*, *42*(5), 1929-1941.
4. Hayashi, I., Panish, M. B., Foy, P. W., & Sumski, S. (1970). Junction lasers which operate continuously at room temperature. *Applied Physics Letters*, *17*(3), 109-111.
5. Gao, H., Luo, D., Ren, Y., Fang, W., Zhou, Y., Liao, J., ... & Liu, B. (2025). The Rise of Colloidal Quantum Well Light Emitting Diodes. *Advanced Functional Materials*, *35*(23), 2422377.
6. Hu, Z., Fu, Q., Lu, J., Zhang, Y., Zhang, Q., Wang, S., ... & Ni, Z. (2024). Van der Waals integrated single-junction light-emitting diodes exceeding 10% quantum efficiency at room temperature. *Science Advances*, *10*(40), eadp8045.
7. Wang, Z., Liu, H., Yang, D., & Bao, L. (2025). Luminous efficiency of InGaN/GaN-based green micro-LED improved by n-side graded quantum wells. *Optics Letters*, *50*(8), 2614-2617. https://opg.optica.org/ol/abstract.cfm?URI=ol-50-8-2614
8. Kong, L., Luo, Y., Wu, Q., Xiao, X., Wang, Y., Chen, G., ... & Yang, X. (2024). Efficient and stable hybrid perovskite-organic light-emitting diodes with external quantum efficiency exceeding 40 per cent. *Light: Science & Applications*, *13*(1), 138.
9. Nowsherwan, G. A., Ali, Q., Ali, U. F., Ahmad, M., Khan, M., & Hussain, S. S. (2024). Advances in organic materials for next-generation optoelectronics: potential and challenges. *Organics*, *5*(4), 520-560.
10. da Silva Candido, L., Barbosa de Brito, E., Corrêa Santos, D., & Vieira Marques, M. D. F. (2025). Advances in polymeric white light-emitting OLEDS for high-efficiency lighting applications. *Journal of Materials Science: Materials in Electronics*, *36*(9), 561.
11. Tawalare, P. K., Lohe, P. P., Nafdey, R., Dhale, S., Ugemuge, N. S., & Moharil, S. V. (2025). Review on white-light-emitting diodes based on nanomaterials. *Canadian Metallurgical Quarterly*, 1-33.
12. Nakayama, Y., Kera, S., & Ueno, N. (2020). Photoelectron spectroscopy on single crystals of organic semiconductors: Experimental electronic band structure for optoelectronic properties. *Journal of Materials Chemistry C*, *8*(27), 9090-9132.
13. Lee, T., Kim, M., Chun, B., Park, G., Yim, S., Yu, S., & Kwak, J. (2024). Recent advances in light outcoupling from quantum-dot light-emitting diodes. *ACS Photonics*, *11*(12), 5050-5060.
14. Deva, L., Stakhira, P., Fitio, V., Guminilovych, R., Bulavinets, T., Stanitska, M., & Volyniuk, D. (2025). Exploring quantum wells in OLED technologies: a comprehensive review of applications and advancements. *Ukrainian Journal of Physical Optics*, *26*(2).
15. Ayobi, A., Mirnia, S. N., Roknabadi, M. R., & Bahari, A. (2019). The effects of MoO3/TPD multiple quantum well structures on the performance of organic light emitting diodes (OLEDs). *Journal of Materials Science: Materials in Electronics*, *30*(4), 3952-3958.
16. Abu-Elmaaty, B. E., Ismail, T., Sabeeh, A. H., & Alshaer, N. (2025, July). Optimizing Light Extraction in RGB OLEDs with Multi-Quantum Well Configurations. In *2025 25th Anniversary International Conference on Transparent Optical Networks (ICTON)* (pp. 1-4). IEEE.
17. Hu, S., Shabani, F., Liu, B., Zhang, L., Guo, M., Lu, G., ... & Liu, C. (2022). High-performance deep red colloidal quantum well light-emitting diodes enabled by the understanding of charge dynamics. *ACS nano*, *16*(7), 10840-10851.
18. Usman, M., Mushtaq, U., Zheng, D. G., Han, D. P., Rafiq, M., & Muhammad, N. (2018). Enhanced internal quantum efficiency of bandgap-engineered green W-shaped quantum well light-emitting diode. *Applied Sciences*, *9*(1), 77.
19. Lee, K. J., Turedi, B., Sinatra, L., Zhumekenov, A. A., Maity, P., Dursun, I., ... & Bakr, O. M. (2019). Perovskite-based artificial multiple quantum wells. *Nano Letters*, *19*(6), 3535-3542.
20. Vakarchuk, I.O. (2004). *Quantum mechanics* (2nd ed.). Ivan Franko National University of Lviv.
21. Fitio, V. M., Yaremchuk, I. Y., Romakh, V. V., & Bobitski, Y. V. (2015). A solution of one-dimensional stationary Schrodinger equation by the Fourier transform. *Applied Computational Electromagnetics Society Journal (ACES)*, 534-539.
22. Barsan, V. (2018). Semiconductor quantum wells with BenDaniel–Duke boundary conditions and Janus nanorods. In AM Al-Ahmadi (Ed.), *Semiconductors – Growth and Characterization*. IntechOpen.

23. Ollivier, H., & de Melo, O. (2025). *Elementary Fourier Optics for Science and Engineering Students*. IOP Publishing.
24. Kimura, H. (2020). Application of classical interpolation theory. In *Linear Circuits* (pp. 61-86). CRC Press.
25. Gray, R. M., & Davisson, L. D. (2004). *An introduction to statistical signal processing*. Cambridge University Press.

Fitio, V., Yaremchuk, I., Shchetinin, M., Hladun, M., Stakhira, P. (2026). The Influence of Quantum Particle Mass on the Discrete Energy Spectrum of Multilayer Structures: A Fourier Transform Approach. *Ukrainian Journal of Physical Optics*, *27*(4), 04034 – 04045.
doi: 0.3116/16091833/Ukr.J.Phys.Opt.2026.04034

Анотація. *Багато оптоелектронних пристроїв містять багатошарові структури з квантовими ямами, зокрема напівпровідникові лазери та світловипромінюючі структури на основі органічних напівпровідників (OLED). Для визначення дискретних рівнів енергії в квантових ямах необхідно розв'язати стаціонарне рівняння Шредінгера. Це має враховувати той факт, що ефективна маса носіїв заряду в різних шарах різна. У статті аналізується структура, що складається з трьох квантових ям різної ширини, в яких ефективні маси носіїв заряду відрізняються. Ми пропонуємо чисельний метод розв'язання рівняння Шредингера в частотній області. Цей метод враховує різні ефективні маси в квантових ямах та бар'єрах. Отримані дискретні рівні енергії порівнювалися з тими, що були розраховані за допомогою методу хвиль де Бройля. Це дозволило визначити параметри чисельного процесу, необхідні для досягнення високої точності. Дослідження показали, що маса частинок у бар'єрах мало впливає на дискретні рівні енергії, тоді як маса частинок у квантових ямах має значний вплив. Чисельні розрахунки показали, що для стрибкоподібної зміни маси частинок на межі яма/бар'єр перша похідна від хвильової функції задовольняє граничні умови Бен-Даніеля -Дюка (BenDaniel-Duke). Модулі хвильової функції в координатній області були побудовані для найнижчих енергетичних рівнів. Це вказує на сильну локалізацію носіїв заряду в квантових ямах.*

Ключові слова: *багатошарові квантові структури, рівняння Шредингера, перетворення Фур'є, хвильовий метод де Бройля, маса квантової частинки*